# Numerical investigation of a geometric unbalanced vertical axis wind turbine new concept

*Ion Malael[1*], Ioana Octavia Bucur[1], Valeriu Dragan[1], Marius Dranca[2], Mihai Chirca[2], Stefan Breban[3]*

[1]*National Research and Development Institute for Gas Turbines COMOTI, 220d Iuliu Maniu, Bucharest, Romania*
[2]*Technical University of Cluj-Napoca, 28 Memorandumului street, Cluj-Napoca, Romania*
[3]*BMEnergy Ltd, 42A Simeria street, Cluj-Napoca, Romania*
**ion.malael@comoti.ro*

**Keywords**: VAWT, CFD, TSR, Torque coefficient, PMG

## Abstract

New trends in sustainable modern urban development involve integrating renewable energy sources within the confined spaces between large buildings. Darrieus type vertical axis wind turbines are ideally suited for this mission, since they do not require (re)orientation with a dominant wind and can be easily scaled. Under the assumption that offsetting blades in the radial direction will allow more space for shed vortices to dissipate, this paper proposes an asymmetric vertical axis wind turbine. The radial asymmetry is aerodynamically balanced by changing the chord of each blade proportionately in order to obtain the same momentum coefficient and avoid vibrations and mechanical failure.CFD unsteady simulations of the flow were carried out by using Ansys Fluent to determine the blade to blade interaction and evaluate the efficiency for different tip speed ratios. The analysis results are represented by the vorticity contours for different blade positions and a 360 degree evolution of the torque coefficient for each blade. To reach the technology readiness level 2, a PMG for wind tunnel model was designed and numerically tested. Through obtain results are graphically represented the generated and rectified voltages, the three phase currents and the electric power generated.

## 1 Introduction

The United Nations document "Sustainable Development Goals", published in 2015, that aims to drive the world towards a development in harmony with nature specifically expresses the right of each individual to have access to affordable, reliable, sustainable and modern energy (Goal 7) [1]. The current trend in energy production is to diversify the energy generation towards alternative solutions that can offer a cleaner and safer way. Although the present solutions, based on hydrocarbon fuels, became cleaner, there will be a certain limit which will not be surpassed. Furthermore, the solution architectures almost reached their performance peak. Therefore it is the moment to strive for alternative solutions. Wind turbines represent viable solutions for modern growth in the energy production sector. Their efficiency is increasing as innovations reach maturity and are implemented. Also, the increasing adaptability of different wind turbine architectures to remote areas can provide clean solutions for the development of small communities. Plus, the cost for this type of energy extraction is relatively small compared to other solutions.

The improvements for these wind turbines were possible due to a strong synergy of different fields like aeronautics, automotive, energy extraction, automation, energy storage and, of course, wind turbine design. There are three main architectural types for wind turbines, which cover a wide range of wind velocities (2 m/s to 14 m/s).For low wind velocity applications vertical axis wind turbines (VAWT) are usually selected[2].

Small wind turbines have a limited market penetration due to low energy yield per swept area and rather high cost per generated electricity [3]. Thus, research efforts should be made in order to mitigate these issues.

One of the most important advantages of VAWTs is their omni-directionality, i.e. their ability to harvest wind energy from all directions. Thus, the complicated yawn and pitch system [4] used for horizontal axis wind turbines (HAWTs) is not needed in this case. Although the problem of negative torque developed by the returning blades is significant [5], a pitch system that can modify the blade angles on the returning path is not feasible yet [6].Regarding VAWTs, Tian et al. propose a passive-pitch shield that would adjust the pitch angle according to the wind directions so that the studied VAWT would generate higher efficiency [7].

There are two types of VAWTs: based on the drag force (Savonius) and based on the lift force (Darrieus). The second one is more commonly used, due to its higher power coefficients, simpler construction and lower manufacturing costs [8]. There are three key parameters that influence the aerodynamic performances of wind turbines: solidity, Reynolds number and the material used to fabricate the blades [9]. To further increase the wind turbines' performances, flow control methods must be developed and implemented.

One such method is represented by creating a slot through a blade[10]. This leads to a local pressure growth which increases the lift force. When designing a slotted blade, it is important to carefully consider the length, width and the inlet

and exit angles of the slot. For example, a new method, where the slot exit is located on the pressure side will force the flow direction in the opposite sense compared to the classical approach, thus altering the pressure distribution on both sides of the airfoil[11].The performance increase using slots varies in literature from 10 to 30% [12] and can also alter the stall margins. The leading-edge micro-cylinder is a method to suppress flow separation even at high angles of attack (AoA) without increasing wind turbine load[13]. Through proper sizing and positioning of the cylinder it is possible to increase blade torque up to approximately 25%.The key aspects of this method are the major impact it has on the Kelvin-Helmholtz flow instability and the flow acceleration it creates on the suction side. The approach also delays the boundary layer detachment at adverse AoAs, conclusion that was also proven by numerical analysis on a VAWT's blade [14].

Another flow control method is the use of Gurney Flap (GF), first used in the car industry to increase the stability of a car at high speeds. Seeing its potential, the aeronautic industry adapted it to its needs [15]. It was discovered that the GF can be used to enhance lift and delay flow separation on an airfoil[16]. Different ways of implementation for the Gurney Flap are experimentally investigated by Maughmer&Bramesfeld [17]. A key parameter is the height of the GF. Liebeck [18] showed that an optimal height is between 1 to 2% of the chord length of the airfoil. Li et al. [19] have shown that at Mach=0.7 even a height of 5% of the chord length determined a 40% increase in lift coefficient. Also, Bianchiniet al et al. [20] discuss the height factor regarding the use of GF, concluding that different GF heights require different angles of attack for an optimal increase in efficiency.

Self-activated movable flaps are only controlled by the flow characteristics around the blade and do not require external control. The difference in pressure above and under the flap triggers the control until equilibrium is reached. This method increases the interval of stable flow regimes by delaying the flow detachment from the blade at adverse AoAs.

Another aspect to be considered is the dissipation of the two counter rotating vortices that form behind the blade. However, there are no studies so far regarding the time needed for these vortices to dissipate. It was found, though, that an increase in lift coefficient is achievable through accelerated dissipation [21].

Leading-edge serration modifies the leading edge to incorporate a system similar to the chevron system. This type of blade generates a series of counter rotating vortices near the leading edge and reduces the flow separation at adverse AoAs. The amplitude of the chevron's teeth can modify the power consumption. For example, at a 0.016m amplitude and a wavelength of 0.09 m the power coefficient can be increased by 16% [22].

A combination between Savonius and Darrieus was developed in order to increase the self-staring capability of a Darrieus wind turbine. This was done by using a J-shaped airfoil. The optimized blade profile is modified on the pressure side towards the trailing edge to reduce the pressure. It was discovered that this method can increase efficiency by up to 20% and reduce torque amplitude [23].The airfoil with cavity concept tries to reduce the flow detachment in adverse conditions [24]. Lasagna et al. [25] managed to demonstrate on a NACA0024 blade profile that this method works only for a small AoA interval ($-2° \leq \alpha \leq 8°$). Their discovery showed that a stable vortex-trapping inside the cavity can be achieved only at high Reynolds numbers, while at low Reynolds numbers the profile behaves worse than the standard geometry. Another flow control method is represented by the use of serrations at the leading edge in order to enhance power. This innovative proposal is better suited for low tip speed ratios (TSRs) according to the 3D numerical study and further studies should be conducted[26].

The electric generator is an important subcomponent of the wind energy conversion system. Several constructive topologies are possible divided in radial flux and axial flux machines [27]. Axial flux machines [28] are a good option for direct-driven operation with the turbine blades [29], as their power density is higher compared with radial flux machines and are more easily built at higher diameters, allowing higher torque for low speed operation. Also, the use of a gearbox is not required.

In the present work, numeric simulations on a reduced scaled model of a new straight-bladed Darrieus concept, were carried out for different tip speed ratios in order to analyse the reduction of the blade to blade flow impact. The proposed solution is presented in Figure 1 and will be described in more detail in section2. This geometry can be considered to be an innovative flow control method.

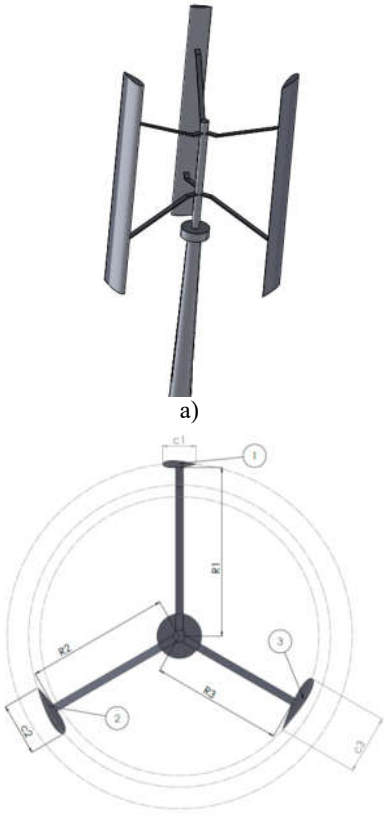

a)

b)

Fig. 1 (a) 3D CAD VAWT concept (b) cross section of the model.

## 2. Methodology

The proposed wind turbine configuration is composed of three straight blades of different chord lengths, placed at 120°of each other, at different radii. The blades have the same NACA 0018 airfoil shape [30] and the VAWT model features are reported in Figure 1.

To select the rotation radius for each blade, a 2D flow modelling was carried out using the Fluent implementation of Menter's k-omega SST with laminar to turbulent transition additional equations [31], further described in [32]. Similar models have been used in wind turbine studies with good results [33]. A pseudo-structured mesh was employed, with 10 chord offset margins, ensuring model stability and resolution while maintaining an acceptable cell count. Considering a sub unity TSR, the resulting free-stream velocity was of 12 m/s, corresponding to the outermost airfoil. Operating total temperature and pressure were set according to the International Standard Atmosphere conditions. Since the turbulence model used to investigate the lift coefficients requires a low y+ value in order to resolve the boundary layer, a summary calculation - based on the local friction coefficient correlation- was carried out, as follows:

$$y_x = \frac{y^+ \cdot \mu}{\rho \cdot u_{*_x}} \quad (1)$$

$$u_{*_x} = \sqrt{\frac{\tau_{w_x}}{\rho}} \quad (2)$$

$$\tau_{w_x} = Cf_x \cdot \rho \cdot \frac{u_{m_x}^2}{2} \quad (3)$$

$$Cf_x = \frac{0.455}{(log_{10} Re_x)^{2.58}} \quad (4)$$

In the end, the first layer height was chosen at a conservative value of one micron, with a growth ratio of 1.1:1. For the highest flow velocity, the y+ values were plotted in Figure 2, in order to check that the model has been correctly implemented.

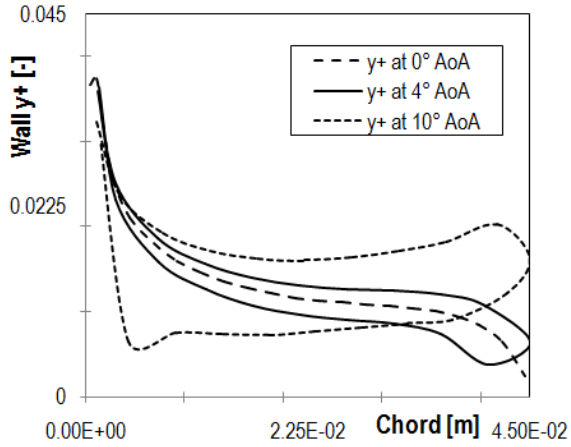


Fig. 2Wall y+ distribution for the outermost airfoil at 12 m/s free-stream velocity

The length of the VAWT's arms supporting the blades is calculated through an iterative process with feedback-loops recalculating the lift coefficient ($C_L$) as a function of the Reynolds number. Initially, each of the Reynolds numbers are estimated from the chord and the tip speed ratio TSR-$V_\infty$ correlation. However, since each arm is envisioned to be different, there will be discrepancies within a reasonable range, hence the need to reiterate the calculations.

The length of the longer VAWT arm was imposed for constructive reasons at 0.2m, while the others were computed using the following equation, ensuring that the overall torque is balanced on all three blades.

$$R_n = R_{ext} \sqrt[3]{\frac{C_{Lext} \cdot C_{ext}}{C_{L\,n} \cdot C_n}} \quad (5)$$

The lift coefficient was calculated as stated above. In the end, the three airfoils tested yielded the following lift polar plots:

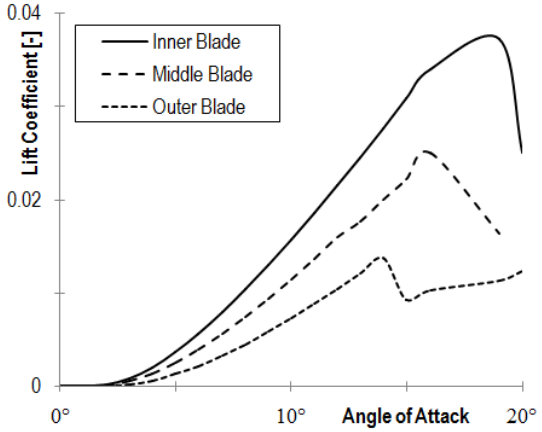


Fig. 3Lift Polar plots of the three airfoils used in the current study

One can see that, due to the Reynolds number difference, even identical airfoils lead to different lift coefficients. Moreover, the stall point is shifted also due to Reynolds effects. The VAWT model geometric characteristics are presented in Table 1.

Table 1. The model features.

| Blade No. | Chord [m] | Length [m] | Diameter [m] | Airfoil type |
|---|---|---|---|---|
| I. Exterior | 0.045 | 0.500 | 0.400 | NACA0018 |
| II. Middle | 0.065 | 0.500 | 0.320 | NACA0018 |
| III. Interior | 0.079 | 0.500 | 0.280 | NACA0018 |

For the VAWT flow investigations a 2D computational domain, further split in two sub-domains (rotor and stator) has been defined. The blades and the shaft were incorporated in the rotor sub-domain where the rotational speed was imposed by using mesh motion option in Ansys Fluent CFD software. Between rotor and stator an interface option was used to interconnect these two sub-domains.

Figure 4 shows the computational domain with the boundary condition for the cases where at inlet the velocity on x direction was imposed, 12m/s.

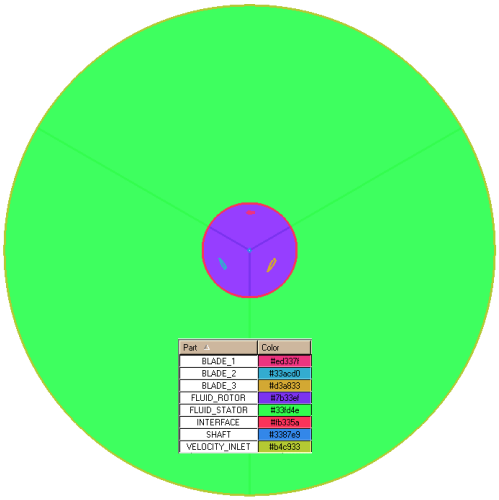


Fig. 4 Computational domain and the BC

In order to have a quad elements structured mesh, the ICEM CFD software with the blocking function was used. Figure 5 shows the blocking structure for the VAWT case where the O-grid structure has been implemented around the walls parts to resolve the probable issues which can appear in the boundary layer regions and Figure 6 shows the mesh.

By using the O-grid structure, the first element near the blades was imposed at $2x10^{-5}$m, condition to get the $y^+$ value around 1.

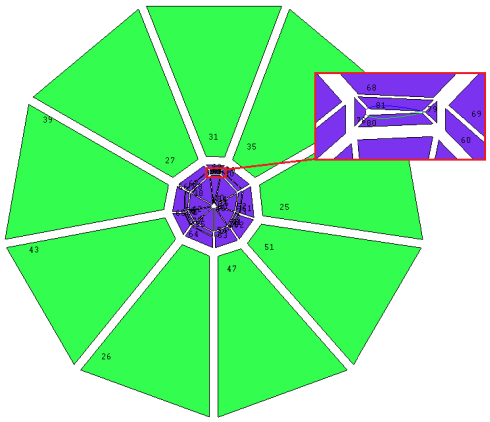

Fig. 5ICEM CFD blocking structure

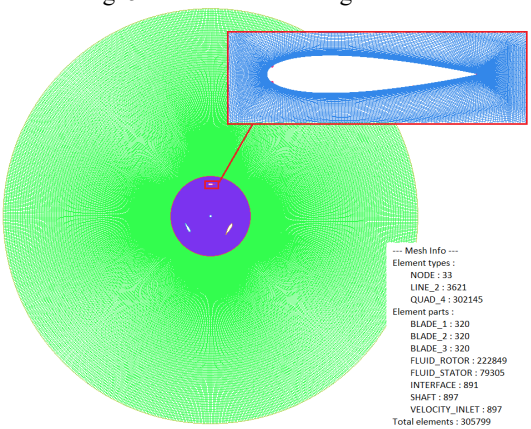


Fig. 6Mesh

At the CFD base stand the Navier-Stokes equations system, which include the equation of continuity, conservation of momentum and conservation of energy. The analyses were carried out by using the Unsteady Reynolds Averaged Navier-Stokes based model SST. This turbulence model is the combination of the standard k-ε model and the k-ω model, using k-ε for the free flow area, which is considered fully turbulent, and the k-ω model for the boundary layer.

The electric generator considered for the application is an ironless two rotor – one stator three phase machine (Figure. 7). The machine has 28 magnetic poles and 21 coils and has been designed for a nominal power of 15 W at 100 RPM. The permanent magnets (PMs) are mounted circumferentially with alternate magnetisation (Figure. 8), on ferromagnetic steel rings (rotor iron disc in Figure. 7). Also, the magnetic flux pathway is presented in Figure. 8.

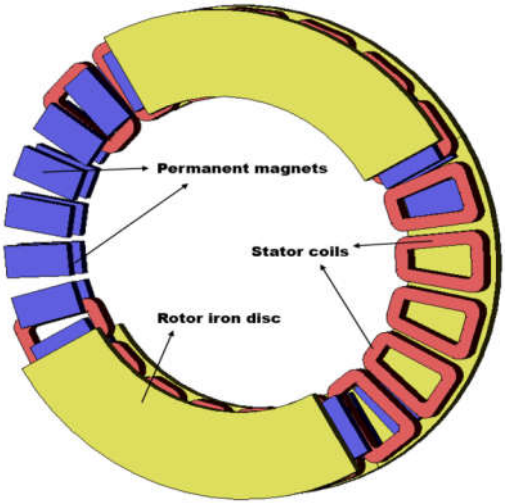


Fig. 7.3D representation of the three-phase coreless AFPMG.

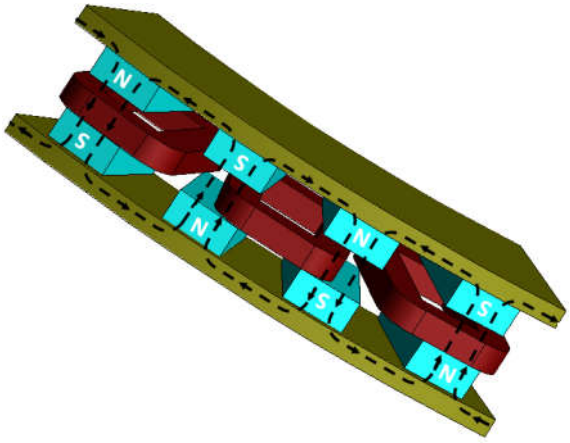


Fig. 8. Magnetic flux pathway.

The simulations of the generator where made using J-MAG FEA software. The generated electric power is rectified and then transferred to a resistive load (Figure. 9).

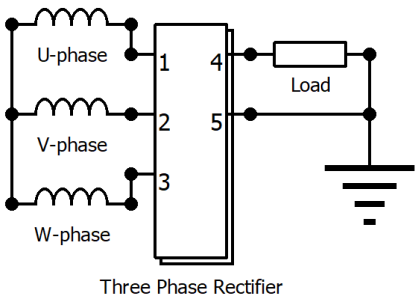


Fig. 9. Electric circuit of the generator

## 3 Results

In order to determine the blade to blade interaction, the vorticity magnitude for different positions of the blade, has been plotted. This makes it easier to observe the evolution of the vortex interaction with the blades, which has a negative impact on the overall performance of the wind turbine. The variations of the torque coefficient were plotted for a period $T=360^0$ for each blade with different TSR values. Figure 11 shows the variation of the torque coefficient for different values of the TSR. The maximum value is obtained at TSR=2.

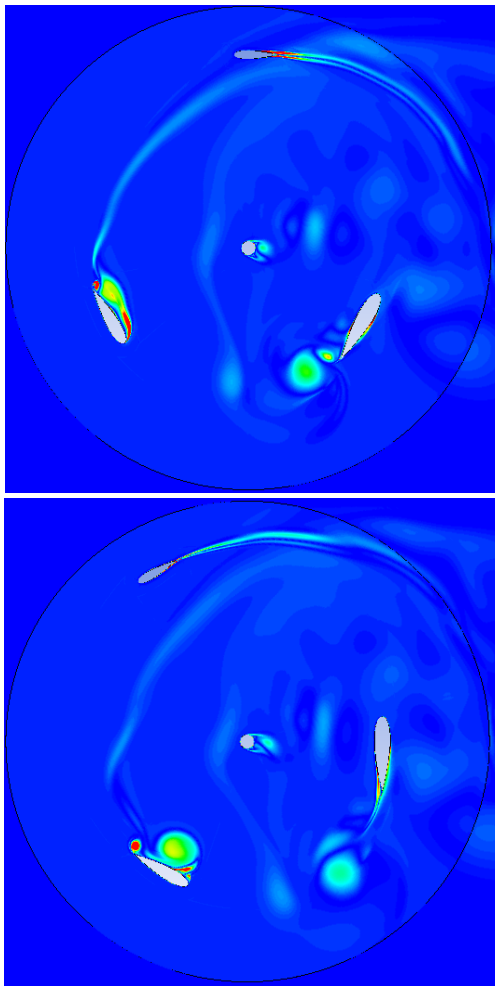


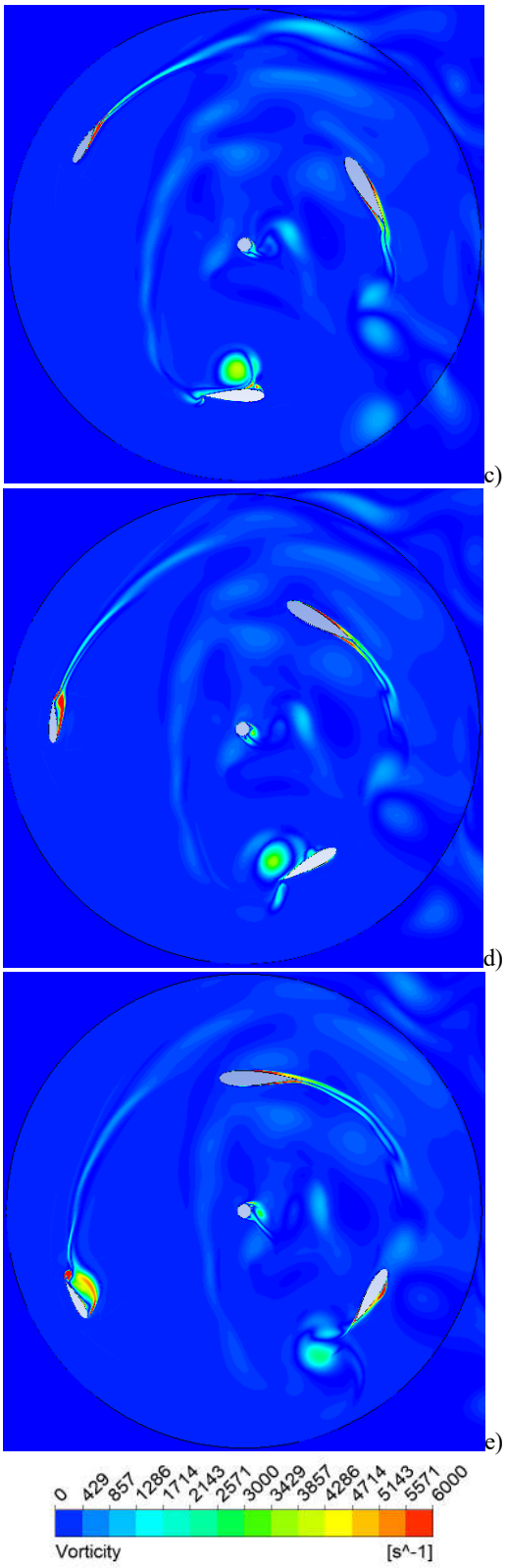


Fig. 10. Vorticity magnitude evolution for TSR=2. a) 0 degree position; b) 30 degree position; c) 60 degree position; d) 90 degree position; e) 120 degree position;

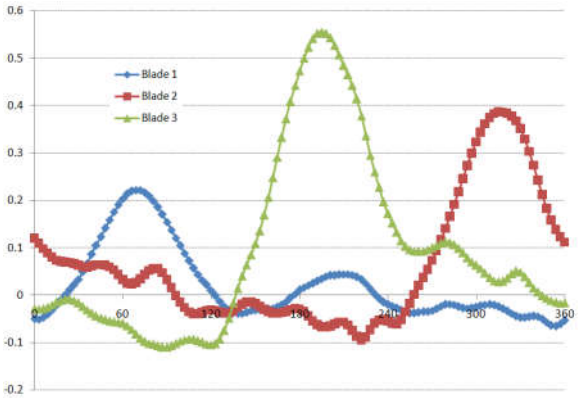


a)

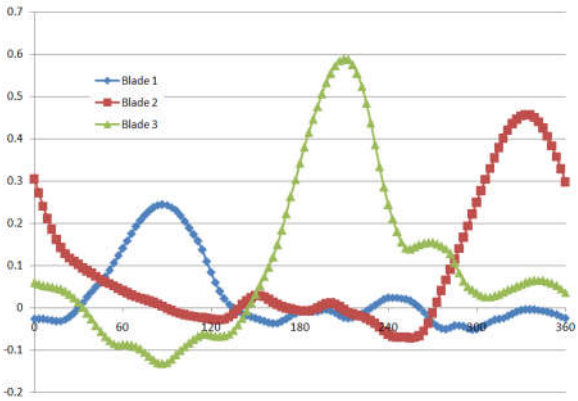


b)

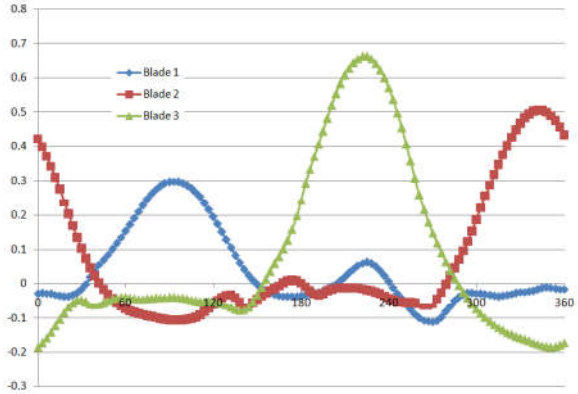


c)

Fig. 11. Torque coefficient variation;
a) TSR=1.2; b) TSR=1.6; c) TSR 2.

In Figs. 12-16 are presented the simulation results. Figs 12 and 13 are showing the voltages and currents generated. Due to the three-phase rectifier, third order harmonics can be observed. This is the reason for the fluctuations of the generated power (Fig. 14). The generator losses are almost entirely caused by Joule losses in the windings, situated at little more than 1.4 W (Fig. 15). The electromagnetic torque oscillates around 1.85 Nm, as shown in Fig. 16.

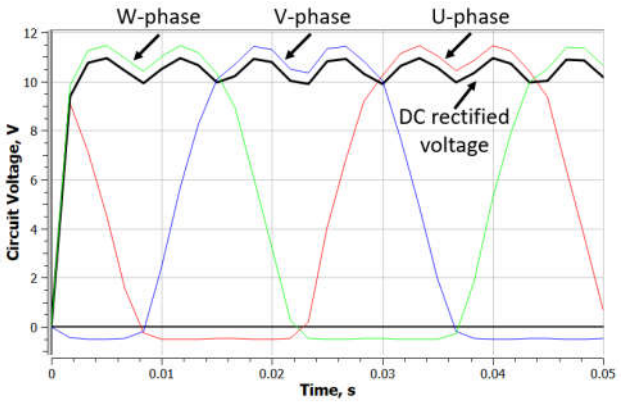


Fig. 12. Generated and rectified voltages.

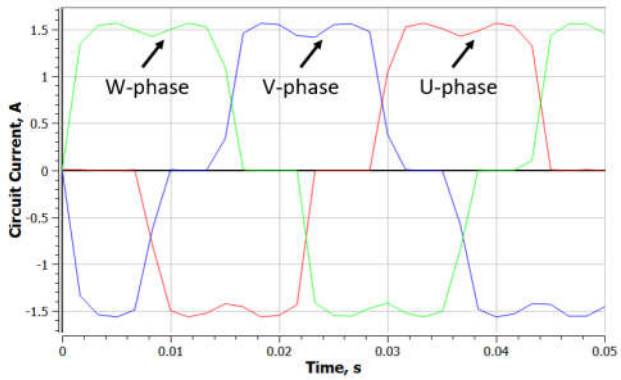


Fig. 13. Three phase currents.

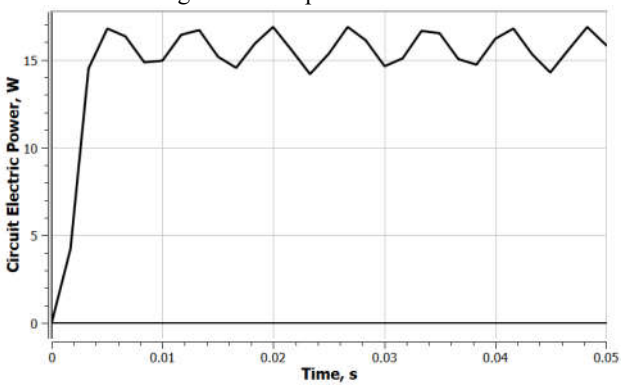


Fig. 14. Electric power generated.

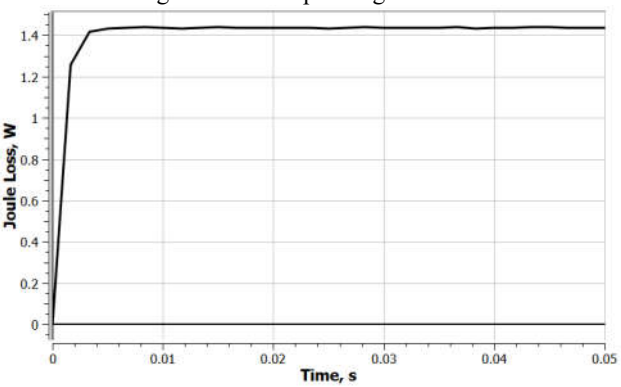


Fig. 15. Joule losses.

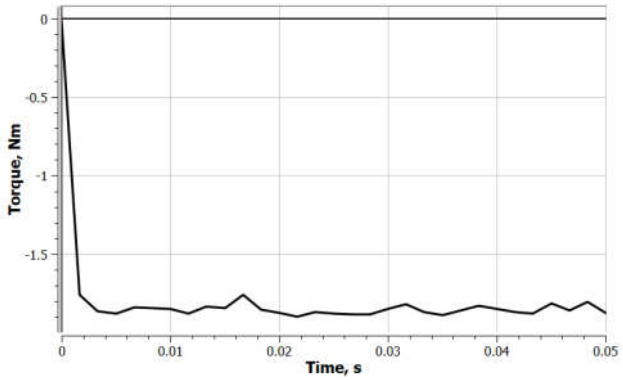

Fig.16. Mechanical torque.

## 4 Conclusion

In this scientific paper, the flow around a new vertical axis wind turbine concept has been numerically investigated by using the CFD methods; in order determine the blade to blade impact. The paper proposes a new model for a VAWT, with blade installation at different radial positions and inversely proportionate chords so that they match their moment. A mathematical model and design procedure arealso provided and validated through the subsequent experiments. The model uses lift coefficients determined through CFD study. In this particular case we reconfigured existing blades and therefore the arm length had to be calculated for each individual blade, based on airfoil and chord. Conversely, the design relations can be used to pre-establish arm lengths and deduce the blade airfoil and chord combination. The theoretical model turned out to be a well-balanced turbine, with little wind induced vibrations.

Future work will also include experimental testing of the concept in a wind tunnel where the flow will be evaluated by using the particle image velocimetry (PIV) technique. Figure 17 illustratesa representative photo of the experimental setup.

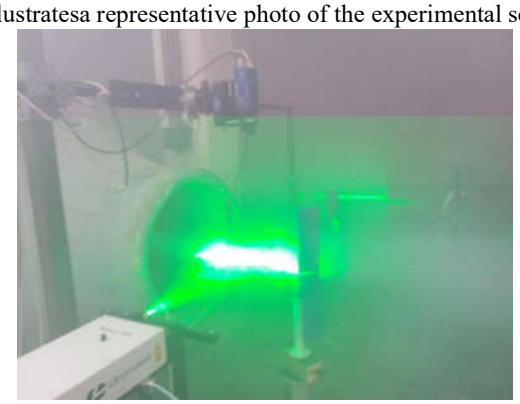
Fig.17. Experimental setup

## 5 Acknowledgements

This work was carried out within POC - Competitiveness Operational Program, supported by the EU and Romanian Minister of Research and Innovation funds, project number POC 9/01.09.2016, Smis 105890, ID P_40_309.

## 6 References

[1]Sustainable Development Goals - Full report of the Open Working Group of the General Assembly on Sustainable Development Goals is issued as document A/68/970, available at http://undocs.org/A/68/970

[2] Eriksson S, BernhoffH, Leijon M.Evaluation of different turbine concepts for wind power. Renewable and Sustainable Energy Reviews, 2008,12, pp. 1419-1434.

[3] Ani S O, Polinder H, Ferreira J A, “Comparison of energy yield of small wind turbines in low wind speed areas”, IEEE Trans. Sustainable Energy, vol. 4, no. 1, pp. 42-49, 2013.

[5] SongD, Yang J, Fan X, Liu Y, Liu A, Chen G, JooYH. Maximum power extraction for wind turbines through novel yaw control solution using predicted wind directions. Energy Conversion and Management, 2018,157, pp.587-599.

[6] Sharifi A, NobariMRH.Prediction of optimum section pitch angledistribution along wind turbine blades.EnergyConversion andManagement, 2013, 67, pp.342-350.

[7] Najafian-AshrafiZ, Ghaderi M, SedaghatA.Parametric studyon off-design aerodynamic performance of a horizontal axis wind turbine blade and proposed pitch control. ECM, 2015, 93, pp. 349-356.

[8] Tian W, MaoZ, Ding H.Numerical study of a passive-pitch shield for the efficiency improvement of vertical axis wind turbines.Energy Conversion and Management, 2019,183, pp. 732-745.

[9] Jafari M, Razavi A, Mirhosseini M. Effect of airfoil profile on aerodynamic performance and economic assessment of H-rotor vertical axis wind turbines. Energy, 2018, 165, 792-810.

[10] Meana-Fernández A, Solís-Gallego I, Oro JMF, Díaz KMA, Velarde-Suárez S. Parametrical evaluation of the aerodynamic performance of vertical axis wind turbines for the proposal of optimized designs. Energy, 2018, 147, 504-517.

[11] Beyhaghi S,Amano RS. Improvement of aerodynamic performance of cambered airfoils using leading-edge slots. Journal of Energy Resources Technology, 2017, 139(5), 051204.

[12] Subash B, NithyapathiC, ManikandanD,MuraliKK. Aerodynamic Optimization of Wind Turbine Blade by Employment of Slot to Counteract the Effect of Drag. Int. J. Emerging Technol. Adv. Eng.,2014,4(3), pp. 249–253.

[2] Burton T, JenkinsN, Sharpe D,Bossanyi E.Wind Energy Handbook - 2nd Edition. John Wiley & Sons, Inc., 2011, Chichester, UK.

[13] Wang, Y, Li G, Shen S, Huang D, Zheng Z. Investigation on aerodynamic performance of horizontal axis

wind turbine by setting micro-cylinder in front of the blade leading edge. Energy, 2018, 143, 1107-1124.
[14] Zhu H, Hao W, Li C, Ding Q,Wu B. A critical study on passive flow control techniques for straight-bladed vertical axis wind turbine. Energy, 2018, 165, pp. 12-25.
[15] ZhuH, HaoW, Li C, DingQ.Numerical study of effect of solidity on vertical axis wind turbine with Gurney flap,Journal of Engineering and Industrial Aerodynamics, 2019, 186, pp. 17-31.
[16] Chandrasekhara MS. Optimum Gurney flap height determination for "lost-lift" recovery in compressible dynamic stall control. Aerospace Science and Technology, 2010,14(8),pp. 551-556.
[17] Maughmer MD,Bramesfeld G. Experimental investigation of Gurney flaps. Journal of Aircraft, 2008, 45(6), pp. 2062-2067.
[18] Liebeck RH. Design of subsonic airfoils for high lift, Journal of Aircraft, 1978, 15, pp. 547-561.
[19] Li YC, Wang JJ,Hua J. Experimental investigations on the effects of divergent trailing edge and Gurney flaps on a supercritical airfoil. Aerospace Science and Technology,2007, 11, pp. 91-99.
[20] Bianchini A, Balduzzi F, Di Rosa D, Ferrara G.On the use of Gurney Flaps for the aerodynamic performance augmentation of Darrieus wind turbines, Energy Conversion and Management, 2019, 184, pp. 402-415.
[21] Schatz M, Knacke T, Thiele F, Meyer R,Hage W,Bechert DW. Separation Control by Self-Activated Movable Flaps. AIAA 2004-1243, 42th AIAA Aerospace Sciences Meeting & Exhibit, 2004.
[22] Hao W, Ding Q, Li C. Optimal performance of adaptive flap on flow separation control. Computers&Fluids, 2019, 179, pp. 437-448.
[23] ZamaniM, Maghrebi MJ,Varedi SR. Starting torque improvement using J-shaped straight-bladed Darrieus vertical axis wind turbine by means of numerical simulation. Renewable energy, 2016, 96, pp. 109-126.
[24] Shi S, New TH, Liu Y. On the flow behaviour of a vortex-trapping cavity NACA0020 aerofoil at ultra-low Reynolds number. In 17th International Symposium on Applications of Laser Techniques to Fluid Mechanics, Lisbon, Portugal, 2014, pp. 07-10.
[25] Lasagna D, Donelli R, De Gregorio F, Iuso, G. Effects of a trapped vortex cell on a thick wing airfoil. Experiments in fluids, 2011, 51(5), pp. 1369-1384.
[26] Wang Z, WangY, Zhuang M. Improvementof the aerodynamic performance of vertical axis wind turbines with leading-edge serrations and helical blades using CFD and Taguchi method,Energy Conversion and Management,2018, 177, pp.107-121.
[27] E. Spooner, A.C. Williamson, "Direct-coupled, permanent-magnet generators for wind turbines", Proc. IEE – Electr. Power Applic., vol. 143, no. 1, pp. 1–8, 1996.
[28] F. G. Capponi, G. De Donato, and F. Caricchi, "Recent Advances in Axial-Flux Permanent-Magnet Machine Technology", IEEE Transactions on Industry Applications, vol. 48, no. 6, November/ December 2012.
[29] T. F. Chan and L. L. Lai, "An Axial-Flux Permanent-Magnet Synchronous Generator for a Direct-Coupled Wind-Turbine System", IEEE Transactions on Energy Conversion, vol. 22, no. 1, March 2007.
[30] Dumitrescu H, Cardoş V, Mălăel I. The physics of starting process for vertical axis wind turbines. In CFD for wind and tidal offshore turbines, Springer, Cham, 2015, pp. 69-81.
[31] Menter FR, Langtry RB, Likki SR, Suzen YB, Huang PG, Volker S. A Correlation-Based Transition Model Using Local Variables: Part I — Model Formulation, ASME-GT2004-53452,2004.
[32] Langtry RB, Menter FR. Correlation-based transition modeling for unstructured parallelized computational fluid dynamics codes. AIAA journal, 2009, 47(12), pp.2894-2906.
[33] Nandi TN, Brasseur J, Vijayakumar G. Prediction and analysis of the nonsteady transitional boundary layer dynamics for flow over an oscillating wind turbine airfoil using the γ-reθ transition model. In 34th wind energy symposium, 2016 (p. 0520).